Published in *J. Low Temp. Phys.* **145**, 311-335 (2006).

Non-Stationary Nonlinear Phenomena on the Charged Surface of Liquid Hydrogen

G. V. Kolmakov[1,2], M. Yu. Brazhnikov[1], A. A. Levchenko[1], A. N. Silchenko[2†], P. V. E. McClintock[2], and L. P. Mezhov-Deglin[1]

[1] *Institute of Solid State Physics RAS, Chernogolovka, 142432, Russia*
[2] *Department of Physics, Lancaster University, Lancaster LA1 4YB, UK*
[†] *Now at: Institute of Medicine, Jülich Research Centre, 52425 Jülich, Germany*

Investigations of nonlinear phenomena on the charged surface of liquid hydrogen are reviewed. It is demonstrated that excitation of the surface by a low frequency ac electric field results in the formation of capillary waves in the high frequency domain, and that the latter exhibit turbulence. The quasi-adiabatic decay of this capillary turbulence has been studied both experimentally and theoretically. It is shown that the processes of formation and decay of the turbulence are both controlled by the same relaxation mechanisms. For spectrally narrow pumping, the application of an additional low frequency driving force causes a decrease of wave amplitude in the high-frequency domain of the turbulent spectrum and correspondingly decreases the width of the inertial range of energy transfer.

PACS: 68.03.Kn; 47.35.+i; 47.27.Gs

1. INTRODUCTION

Experiments over the last ten years have revealed many interesting nonlinear phenomena[1–14] associated with wave motion on the charged surface of liquid hydrogen. In what follows we present a succinct review of this work, summarising the most important observations and their interpretation, and including a discussion of our most recent experimental and theoretical results. The basis of the experiment is illustrated schematically in Fig. 1. A laser beam is reflected from the charged surface of liquid hydrogen. Dc and ac electric fields are applied between the charged layer and a conical electrode placed above the liquid. Further details of the experimental arrangement and the procedures used are given in Sec. 3. We review the theoretical

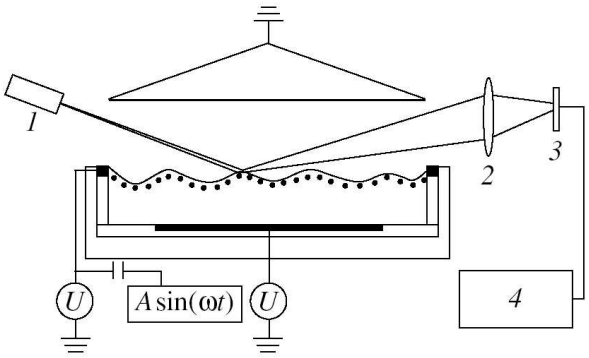

Fig. 1. Schematic view of the experimental cell: (1) laser, (2) lens, (3) photodetector, (4) analog-to-digital converter.

background in Sec. 2. We present and discuss the main experimental and theoretical results in Secs. 4. and 5. First, however, we consider the properties to be expected of waves on a charged surface and we introduce the concept of wave turbulence.

1.1. Waves on the charged surface of liquid hydrogen

The dispersion law for surface waves on a flat, equipotential, charged layer of liquid between the plates of a horizontal capacitor can in general be written as[15]

$$\omega_k^2 = k \tanh(kh) \left(g + \frac{\alpha k^2}{\rho} - \frac{2kP}{\rho} \coth(kd) \right), \tag{1}$$

where ω_k is the frequency of a wave of wave vector k, h is the thickness of the liquid layer, α is the surface tension, ρ is the density of the liquid, g is the acceleration due to gravity, d is the distance between the surface and the upper plate of the capacitor, $P = U^2/8\pi d^2$ is the equilibrium pressure of the electric field on the surface, and U is the voltage applied to the capacitor (note that the electric force acting on the charged surface is directed upwards, oppositely to the gravitation force).

In the case when the distance from the surface to the control (upper) electrode is smaller than the wavelength ($kd \leq 1$), the dispersion law (1) for surface waves on a deep liquid simplifies greatly and can be written as

$$\omega_k^2 = k \left(G + \frac{\alpha k^2}{\rho} \right), \tag{2}$$

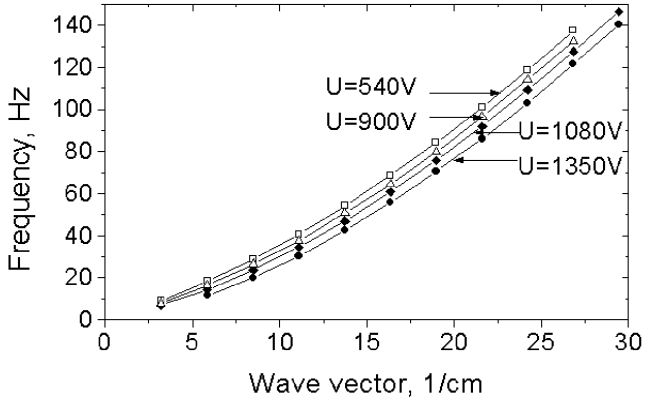

Fig. 2. Spectrum of oscillations of the charged surface of liquid hydrogen in the cylindrical cell for different values of the capacitor voltage U below the second critical voltage U_2.

where the quantity $G = g - 2P/\rho\, d$ acts as an effective acceleration due to gravity.

If the applied voltage tends to the critical value $U_{c1} = (4\pi\rho d^3)^{1/2}$, the effective gravitational acceleration $G \to 0$, and the effective capillary length $\lambda_{\text{eff}} = 2\pi(\alpha/\rho G)^{1/2} \to \infty$. In this case the surface waves can be considered as being purely capillary waves at *all* values of k, even where the wavelength exceeds the capillary length of a neutral liquid $\lambda = 2\pi(\alpha/\rho g)^{1/2}$. Hence $\omega_k \propto k^{3/2}$ at practically all k.

From equation (2) it follows that in high electric fields $U > U_{c1}$, where the effective acceleration due to gravity G becomes negative, a flat charged surface should be unstable against a perturbation with $k \leq \sqrt{\rho|G|/\alpha}$. We have observed this instability (reconstruction of the initially flat charged surface of liquid hydrogen) experimentally[2]: at voltages $U > U_{c1}$ a stationary solitary wave (a hump) forms on the surface in a cylindrical cell filled with liquid hydrogen. A similar phenomenon – formation of a stationary dimple – was observed on the negatively charged surface of liquid helium[2]. It should be mentioned that, as the voltage increased above a second critical voltage[3,4], $U_{c2} \simeq 1.2\, U_{c1}$, the reconstructed surface of the liquid hydrogen lost stability and a discharge pulse occurred from the top of the hump: it looked like a geyser. After this discharge, the surface relaxed to its original flat state and then the process repeated. Because of this effect, it was in practice impossible to study capillary waves on the reconstructed surface of liquid hydrogen at voltages above $1.2U_{c1}$. After stepwise switching on the voltage U higher the third critical voltage $U_{c3} > U_{c2}$ the extraction of charges from under the

surface of liquid hydrogen was observed[1]. In this regime the charged clusters (snowballs) moved by strong electrical force penetrate through the liquid-vapor interface, and a steady-state electrical current through the surface is established.

Dispersion curves $\omega(k)$ for oscillations of the charged surface are shown in Fig. 2. The first critical voltage in these measurements $U_{c1} = 1200$ V, the second critical voltage $U_{c2} = 1440$ V, and the temperature was 15 K. As can be seen in the figure, the spectrum is close to $\omega(k) \sim k^{3/2}$; with increasing voltage the spectrum softens and no particular changes were observed in fields higher than the first critical value. As pointed out in Refs. 2,3 the observed reconstruction can be discussed in terms of a second order phase transition corresponding to a softening of the spectrum of surface waves with increasing external electric field, as illustrated in Fig. 2.

1.2. Wave turbulence on liquid hydrogen

A highly excited state of a system with numerous degrees of freedom, characterised by the presence of an energy flux that is directional in K-space, is referred to as *turbulent*. In its turbulent mode, a system is far away from its thermodynamic equilibrium and is characterised by significant nonlinear interaction of the degrees of freedom, as well as by the dissipation of energy[16,17]. The nonlinear interaction brings about an effective redistribution of energy between the degrees of freedom (modes). Turbulence may be observed in systems where the frequencies of excitation (energy pumping) and energy dissipation are widely spaced in frequency.

Studies of energy propagation in such systems have included capillary waves on the surface of liquid, which are of great interest from the standpoint of both fundamental nonlinear physics and practical applications. The theory of weak, or wave, turbulence was developed in the late 1960s (see the monograph[17] and references therein). However, despite many experimental investigations of the nonlinear dynamics of surface waves, only a few experimental observations of isotropic spectra of capillary waves on the surface of water have been reported[20–23], the results of which might be compared with the theoretical predictions.

We review below the results of our recent investigations[5–14] of nonlinear capillary waves on the surface of liquid hydrogen. Liquid hydrogen is an especially suitable object for such experiments because it is characterised by relatively low values of density ρ and kinematic viscosity ν, and by a high value of the coefficient $V \propto (\alpha/\rho^3)^{1/4}$ that describes the nonlinearity of capillary waves. For hydrogen at a temperature $T = 15$ K, it is known

that $\alpha = 2.7$ dyn/cm, $\rho = 0.076$ g/cm^3, $\nu = 2.6 \times 10^{-3}$ cm^2/s and $V = 9$ cm$^{3/4}$/sg, and the capillary length $\lambda = 1.2$ cm. For water at $T = 293$ K, $\alpha = 77$ dyn/cm, $\rho = 1.0$ g/cm^3, $\nu = 10^{-2}$ cm^2/s, $V = 3$ cm$^{3/4}$/sg, and $\lambda = 1.8$ cm which is not so different. This enables us to examine the turbulent mode in liquid hydrogen in a cell with the inner diameter of a few centimetres over a wide frequency range from 10 Hz to 10 kHz. In addition, on account of the low density, the external force required to excite oscillations on the surface of liquid hydrogen is several times less than that in the case of water. This fact proved to be decisive when exciting waves on the surface by means of electric forces. Previous experiments had revealed[1] that one can charge the surface of liquid hydrogen with charges injected initially into the bulk of the liquid, hold the charges in the vicinity of the surface for a long period of time, and excite surface waves using ac electric field. An important advantage of this procedure for the observation of capillary turbulence is the possibility of directly affecting the surface of a liquid by an external force, virtually without acting on the bulk of the liquid, as well as the high degree of isotropy of the exciting force, enabling one to study the turbulence under well-controlled experimental conditions.

2. THEORETICAL BACKGROUND

Capillary waves on the surface of a liquid represent an example of a nonlinear interacting system. The theory of homogeneous capillary turbulence was described by Zakharov and Filonenko[19] who showed that an ensemble of weakly interacting capillary waves may be described within a kinetic equation, similar to the Boltzmann equation of gas dynamics.

The evolution with time t of the occupation numbers $n_{\mathbf{k}} = \langle a_{\mathbf{k}}(t) a^*_{\mathbf{k}}(t) \rangle$ for capillary waves, where $a_{\mathbf{k}}(t)$ is the time-dependant canonical amplitude of the wave with the wave vector $\mathbf{k}$, is described by the kinetic equation

$$\frac{\partial n_{\mathbf{k}}}{\partial t} = St(n_{\mathbf{k}}) - 2\gamma_{\mathbf{k}} n_{\mathbf{k}} + F_{\mathbf{k}}(t). \tag{3}$$

The canonical amplitudes of the waves are expressed via the space Fourier components of the liquid surface elevation $\eta_{\mathbf{k}}(t)$ and of the fluid velocity potential $\Psi_{\mathbf{k}}(t)$ taken at the liquid surface, as follows[18,19]

$$a_{\mathbf{k}} = \sqrt{\frac{\alpha k^2}{\omega_k}}\, \eta_{\mathbf{k}} + i \sqrt{\frac{\rho k}{2\omega_k}}\, \Psi_{\mathbf{k}}. \tag{4}$$

The collision integral in Eq. (3) is equal to

$$St(n_{\mathbf{k}}) = \int d\mathbf{k}_1 d\mathbf{k}_2 \left(R_{\mathbf{k},\mathbf{k}_1,\mathbf{k}_2} - R_{\mathbf{k}_1,\mathbf{k},\mathbf{k}_2} - R_{\mathbf{k}_1,\mathbf{k}_2,\mathbf{k}} \right).$$

Here,

$$R_{\mathbf{k},\mathbf{k}_1,\mathbf{k}_2} = \pi |V_{\mathbf{k},\mathbf{k}_1,\mathbf{k}_2}|^2 \delta(\mathbf{k}-\mathbf{k}_1-\mathbf{k}_2)\delta(\omega_{\mathbf{k}}-\omega_{\mathbf{k}_1}-\omega_{\mathbf{k}_2}) \times \left[n_{\mathbf{k}_1} n_{\mathbf{k}_2} - n_{\mathbf{k}} n_{\mathbf{k}_1} - n_{\mathbf{k}} n_{\mathbf{k}_2}\right],$$

$$V_{\mathbf{k},\mathbf{k}_1,\mathbf{k}_2} = \left(\frac{1}{8\pi}\right)\left(\frac{\alpha}{4\rho^3}\right)^{1/4}\left[(\mathbf{k}_1\mathbf{k}_2 + k_1k_2)\left(\frac{k_1k_2}{k}\right)^{1/4} + (\mathbf{k}\mathbf{k}_1 - kk_1)\left(\frac{kk_1}{k_2}\right)^{1/4} + (\mathbf{k}\mathbf{k}_2 - kk_2)\left(\frac{kk_2}{k_1}\right)^{1/4}\right]$$

is the amplitude of the nonlinear interaction between capillary waves, $\gamma_{\mathbf{k}} = 2\nu k^2$ is the viscous damping coefficient for capillary waves, and $F_{\mathbf{k}}(t)$ is the external driving force.

The main problem in the investigation of wave turbulence is that of finding the energy distribution law in terms of frequency, i.e. the stationary spectrum of the turbulent energy E_ω. The energy E per unit surface of liquid may be written in the form

$$E = \int \omega_k n_k d\mathbf{k} = \int E_\omega d\omega, \tag{5}$$

where ω_k is the frequency of a wave with the vector $\mathbf{k}$. The capillary wave dispersion law

$$\omega = (\alpha/\rho)^{1/2} k^{3/2} \tag{6}$$

is of the decay type ($\omega'' > 0$). The main contribution to the wave interaction is therefore made by three-wave processes, such as the decay of a wave into two waves with conservation of the overall wave vector and overall frequency, as well as the reverse process of the confluence of two waves into one wave. For a system of capillary waves on the surface of a liquid, there exists a so-called *inertial* frequency range in which the energy distribution E_ω has the power-law-like form

$$E_\omega \sim \omega^s.$$

Here s is an exponent that can be estimated from experimental results.

The inertial range is limited from below by the pumping frequency ω_p, and at high frequencies by viscous damping. According to the currently accepted theory[17,19], when the surface of a liquid is excited at low frequencies within a fairly wide band $\omega_p \pm \Delta\omega$ ("wide-band pumping", $\Delta\omega \approx \omega_p$), there is a constant energy flux Q towards high frequencies, i.e. a direct cascade in K-space. The theory of homogeneous capillary turbulence predicts the power law dependence on frequency for the wave distribution function n_k

and the energy distribution E_ω (Kolmogorov spectrum) within the inertial range, which corresponds to

$$n_k = AQ^{1/2}\rho^{3/4}\alpha^{-1/4}k^{-17/4} \tag{7}$$

in terms of k. Here A is a numerical coefficient. The distribution is an exact solution of the kinetic equation (3) in the inertial range of frequencies, where direct excitation of waves by driving is absent, $F_{\mathbf{k}} = 0$, and viscous loss is so small that it can be neglected[19].

The steady-state distribution of the energy of surface waves in the inertial range may also be equivalently described in terms of the pair correlation function in the Fourier representation

$$I_\omega = \langle|\eta_\omega|^2\rangle) \tag{8}$$

of a departure of the surface from the planar state $\eta(r,t)$. From the experimental standpoint, it is most convenient to investigate the correlation function I_ω rather than the energy distribution E_ω, because the deviations of the surface from the planar state $\eta(r,t)$ can be measured directly. When surface oscillations are excited over a wide frequency range, the correlation function is predicted by the theory[17–19] to be

$$I_\omega = \text{const} \times \omega^{-17/6}. \tag{9}$$

Here the dispersion law (6) was used for changing the representation from K-space to ω-space. The theoretical prediction of relation (7) is supported by the results of numerical calculations of the evolution of nonlinear capillary waves, performed directly from the first principles using the hydrodynamic equations[24,25].

In the case of "narrow-band pumping" ($\Delta\omega < \omega_p$), it was demonstrated by numerical calculations in Ref. 27 that a system of equidistant spectral peaks is formed on the I_ω curve at multiples of the pumping frequency. The frequency dependence of the peak height is described by a power-law-like function with an exponent of $(-7/2)$,

$$I_\omega = \text{const} \times \omega^{-7/2}. \tag{10}$$

Note that the relations (9) and (10) were derived for systems of capillary waves with continuous spectra of wave vectors, i.e. for an idealised infinite surface of liquid. The limited size of an actual experimental cell means, however, that the $\omega(k)$ spectrum must in reality be discrete. This fact must be taken into account when comparing the real correlation function with theoretical prediction. The effect of discreteness decreases with increasing

frequency ω because the resonance width, determined by the quality Q factor and by nonlinear broadening of the resonance, increases faster than the distance between the resonances: the spectrum becomes quasi-continuous. In Refs. 25,26 the authors used numerical methods to demonstrate that a discrete system of resonances at a fairly high level of excitation can be well approximated as a quasi-continuous one.

As already mentioned above, the inertial range is limited at high frequencies by a change in the dominant mechanism of energy transfer, from nonlinear wave transformation to viscous damping. The high-frequency edge of the inertial range (boundary frequency) can be defined as the frequency ω_b at which the viscous damping time τ_v becomes comparable in order of magnitude with the characteristic time τ_n of nonlinear interaction (the kinetic relaxation time in the turbulent wave system), $\tau_v \sim C\,\tau_n$, where C is some dimensionless constant. The time τ_n is defined by the parameters of the liquid, as well as by the capillary wave distribution function $n(\omega)$, and may be estimated as

$$1/\tau_n \sim |V_k|^2 n_k k^2/\omega_k = |V_\omega|^2 n(\omega) \tag{11}$$

where $V_\omega = \alpha^{-1/2}\omega^{3/2}$ is the coefficient of interaction of three capillary waves, whose frequencies are close to each other. The value of τ_n defines the characteristic timescales for the relaxation of perturbations over the cascade. It is known[16] that the viscous damping time of capillary waves decreases with increasing frequency as

$$1/\tau_v = 2\nu\omega^{4/3}(\alpha/\rho)^{2/3}. \tag{12}$$

Relations (11) and (12) enable us to derive the dependence of the wave frequency ω_b on the wave amplitude η_p at the pumping frequency ω_p (narrow pumping)

$$\omega_b \sim \eta_p^{4/3}\omega^{23/9}. \tag{13}$$

The values of the exponents in this equation correspond to the frequency dependence of the correlation function[27]

$$I_\omega \propto \eta_p^2(\omega/\omega_p)^{-7/2}. \tag{14}$$

Our investigations have shown[5] that a power law dependence on frequency is observed for the correlation function in the frequency range from 100 Hz to 10 kHz when the charged surface of liquid hydrogen is excited by an external periodic electric force at the resonance frequency of the cell. In this case, the exponent in the correlation function was close to (-3.7 ± 0.3). When the surface was excited simultaneously at two resonant frequencies, the exponent decreased in magnitude and amounted[6] to (-2.8 ± 0.2).

The boundary frequency of the upper edge of the inertial range was determined experimentally for the first time in Ref. 7. As the wave amplitude η_p at the pumping frequency ω_p increases, the boundary frequency is found to shift towards high frequencies according to the power law (13), with an exponent 4/3, as is to be expected when pumping in a narrow band[9].

Quasi-adiabatic decay of capillary turbulence was observed experimentally in Refs. 10,11, and it was investigated theoretically and numerically in Ref. 14. Comparison of these results with the observations of the capillary turbulence formation process[12] have shown that the formation of turbulence, and its decay, are controlled by the same relaxation mechanisms.

For the case of spectrally narrow pumping, it was found[13] that, after an additional low frequency pumping was switched on, the wave amplitude in the high-frequency part of the turbulent spectrum decreased and that the inertial frequency range consequently became narrower. Inversely, after switching off the additional low frequency pumping the inertial range expands to higher frequencies. The damping is caused by an increase of number of the wave modes (harmonics) involved in the nonlinear energy transfer from the low- to the high-frequency domain, and by the redistribution of wave energy among these modes.

3. EXPERIMENTAL PROCEDURE

Experiments were performed in the optical cell located within a helium cryostat[8]. The arrangement is shown schematically in Fig. 1. The cell contains a horizontal plane capacitor. A radioactive plate was located on the bottom capacitor plate. Hydrogen was condensed into a cup formed by the bottom capacitor plate and a guard ring. In the preliminary experiments, the cylindrical container was of diameter 25 mm, depth 3 mm (the narrow cell). Most of the data presented here were obtained from a wider cell with a container 60 mm in diameter and 6 mm in depth. The gap between the fluid surface and the capacitor plate was 4 mm in both cells. The temperature of the liquid was held at 15.5 K.

The free surface of liquid was charged as the result of β-particle (electron) emission from the radioactive plate located in the bulk of the liquid. These electrons ionised a thin layer of liquid in the vicinity of this plate. A dc voltage U was applied between the capacitor plates. Its polarity determined the sign of the charge that formed a quasi-two-dimensional layer below the surface of the liquid. In these experiments, the oscillation of a positively charged surface was studied. The metal guard ring around the radioactive plate prevented escape of charge from under the surface to the

container walls. Oscillations of the surface of the liquid hydrogen (standing waves) were excited by application of an ac voltage to the guard ring at one of the resonant frequencies, in addition to the dc voltage. These oscillations were detected through variations of the power of a laser beam reflected from the surface. The reflected light was focused by a lens onto a photodetector. The voltage across the photodetector was directly proportional to the beam power $P(t)$. It was digitized with the aid of a high-speed 12- or 16-bit analog-to-digital converter, and recorded over several seconds duration onto the hard disc of a computer. We analysed the frequency spectrum P_ω of the total power of the reflected laser beam, which was obtained by Fourier transformation in time of the $P(t)$ dependence recorded.

The laser beam used in the experiments was ∼0.5 mm in diameter, and was incident on the surface of the liquid at a grazing angle of about 0.2 rad. The major and minor axes of the elliptical light spot on the surface of the liquid were 2.5 and 0.5 mm. The procedures for excitation of surface oscillation and its recording, as well as the procedure used for processing the experimental data, are described in Ref. 8. As pointed in that paper, given this size of light spot, the square of the Fourier amplitude of the signal measured for frequencies above 50 Hz is directly proportional to the correlation function in the frequency representation, $I_\omega \sim P_\omega^2$.

4. EXPERIMENTAL RESULTS

4.1. Free Decay of Capillary Turbulence

In this Section, we describe experiments on the decay of turbulent oscillations of the charged surface of liquid hydrogen after a steplike switching-off of the harmonic pumping, and the resultant change in the correlation function I_ω.

The surface waves were excited by harmonic pumping at a fixed frequency ω_p for ∼10 s, which was sufficient to establish a steady-state turbulent distribution in the system of capillary waves. The pumping was then switched off, and the relaxation of free surface oscillations with time was observed. The time of observations was varied from 2 to 10 s. Measurements were carried out for various pump frequencies $\omega_p/2\pi$ in the range from 20 to 400 Hz.

In Fig. 3, sections of the time-dependent photodetector signals $P(t)$ recorded at a pump frequency of (a) $\omega_p/2\pi = 98$ Hz in the narrow cell and (b) 97 Hz in the wide cell are shown. The harmonic pumping is switched off at time $t = 0$, and the oscillation amplitude then starts to decrease. The low-frequency modulation of the signals shown in Fig. 3 is due to uncontrolled

surface oscillations attributable to cryostat vibrations. One can see in Fig. 3 that the decay in the narrow cell proceeds appreciably faster than in the wide one. Clearly, the specific energy loss by friction on the container bottom and walls is much stronger than in the wide cell. For this reason, the detailed measurements of the relaxation processes were carried out with the wide cell.

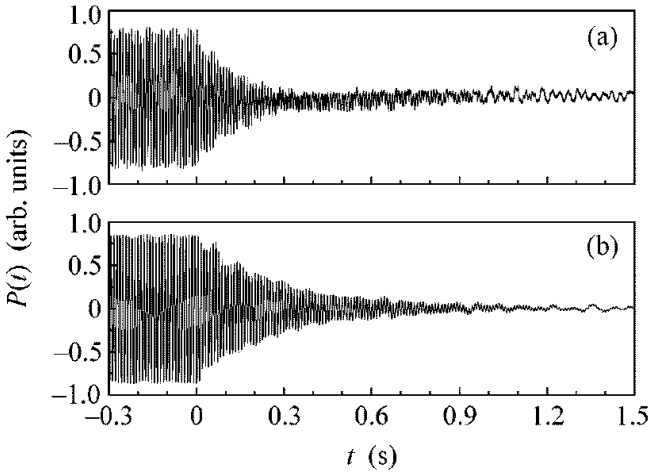

Fig. 3. Relaxation of the liquid-hydrogen surface oscillations after switching off the pumping at frequency $\omega_p/2\pi$ at time $t = 0$: (a) narrow cell with $\omega_p/2\pi = 98$ Hz; and (b) wide cell with $\omega_p/2\pi = 97$ Hz.

In Fig. 4, the time dependences of the signal amplitudes $P(t)$ for pump frequencies of (a) 97 and (b) 173 Hz are obtained by averaging the absolute value of $P(t)$ over a time interval that is a multiple of a half-period of the fundamental frequency. It turned out that the decrease in signal amplitude with time after switching off the pumping can be described by an exponential law $P(t) \sim \exp(-t/\tau)$, where the time constant is equal to $\tau = (0.3 \pm 0.03)$ s for the frequency $\omega_p/2\pi = 97$ Hz and is near twice shorter, $\tau = (0.15 \pm 0.02)$ s, for a pump frequency of 173 Hz.

To study the time evolution of the spectrum I_ω of the correlation function, we used the short-time windowed Fourier transform procedure[28], which is applicable because the experimentally observed signal time decay is much longer than the period of the harmonic force exciting the surface; i.e. $\tau \gg 2\pi/\omega_p$. This allows the choice of a time window with a size smaller than the signal time decay but much larger than the period of the exciting force. By shifting the window position in time, we succeeded in studying the evolution of the turbulent cascade after switching off the pumping. The surface oscillation spectra P_ω^2 for a pump frequency of 97 Hz are shown in Fig. 5 at

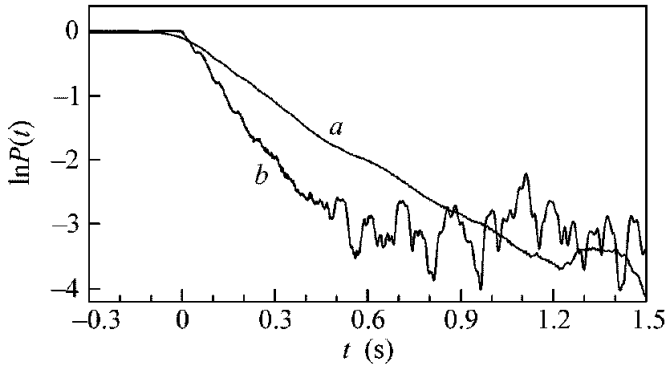

Fig. 4. Time dependence of the signal amplitude $P(t)$ recorded in the wide cell. The pump frequency $\omega_p/2\pi$ was (a) 97 and (b) 173 Hz.

various instants of time after switching off the pumping: after (a) 0.031, (b) 0.49, and (c) 1.07 s.

Immediately after switching off the pumping, the spectrum $I_\omega \sim P_\omega^2$ of the correlation function (Fig. 5a) is still close to the steady-state distribution of the nonlinear surface oscillations during the narrow-band pumping[9]. The fundamental peak is positioned at the pump frequency of 97 Hz, while the higher harmonics form a cascade whose peak heights are described by a power-law frequency dependence $P_\omega^2 \sim \omega^{-3.5}$. The arrow indicates the position of the high-frequency edge $\omega_b \approx 5$ kHz of the inertial range. At time $\Delta t = 0.49$ s after switching off the pumping (Fig. 5b), the wave amplitude at frequency ω_p has decreased by approximately a factor of 3, as compared to Fig. 5a, while the boundary frequency ω_b has decreased to ≈ 2 kHz. The final decay stage after $\Delta t = 1.07$ s, when only a few harmonics are excited, is shown in Fig. 5c. It is remarkable that, over a rather long time interval $\Delta t \leq 0.6$ s after switching off pumping, the high-frequency portion of the spectrum can be described by the distribution $P_\omega \sim \omega^{-3.5}$, which is typical of the steady-state cascade; i.e. the shape of the spectrum is retained during vibrational relaxation, but the oscillations start to decay on the high-frequency domain of the spectrum.

This observation of a quasi-stationary spectrum over a rather long time after switching off the pumping allows one to infer that the nonlinear-interaction time of the capillary waves is much shorter than the viscous-damping time of a linear wave at the pump frequency ω_p. This must still be the case, even where the surface-oscillation amplitude at pump frequency $\omega_p/2\pi = 97$ Hz has become one order of magnitude smaller than its initial value: it decreases from 0.02 mm 0.03 s after switching off pumping to 0.002 mm after 0.6 s (Figs. 5a,b). As a result, the relatively intense energy exchange between

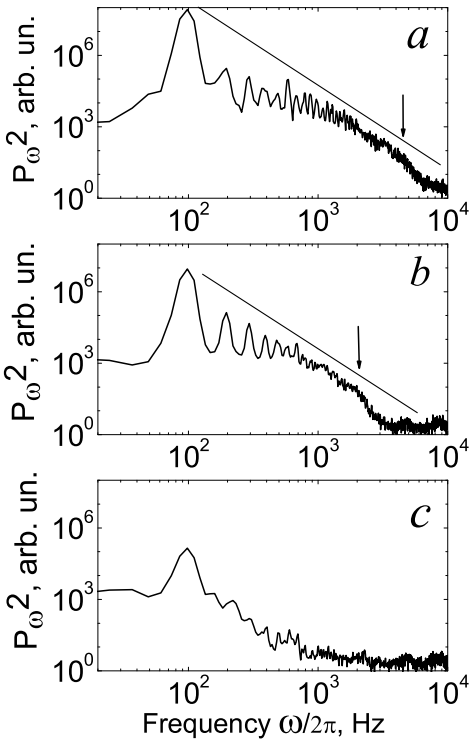

Fig. 5. Instantaneous spectra of the liquid-hydrogen surface oscillations in the wide cell at different times after switching off the pumping at frequency $\omega/2\pi = 97$ Hz: after $\Delta t =$ (a) 0.031, (b) 0.49, and (c) 1.07 s. The solid line corresponds to the power law $P_\omega^2 \sim \omega^{-7/2}$. The arrows in plots (a) and (b) mark the position of the high-frequency edge ω_b of the inertial range.

waves with frequencies lying in the inertial range results in a stabilisation of the power-law spectrum in the low-frequency region $\omega < \omega_b$. At the same time, it follows from the experiment (see Fig. 5 and Fig. 7 below) that the characteristic relaxation time of surface oscillations is determined by the viscous damping of waves at the pump frequency, and decay of the cascade is accompanied by a shift of the high-frequency edge ω_b of the inertial range towards lower frequencies. Hence, when describing the relaxation of nonlinear fluid-surface oscillations within the framework of the kinetic equation (3), one should not ignore viscous loss even at larger surface-oscillation amplitudes. For our experiment these correspond to $k\eta_p \leq 0.04$ rad, or $\eta_p \leq 0.02$ mm for a pump frequency of 97 Hz.

4.2. Formation of Capillary Turbulence

Fig. 6 shows the instantaneous spectra P_ω^2 calculated for times (a) $t =$ 0 s, (b) $t = 0.58$ s and (c) $t = 1.51$ s after switching on the driving force at a frequency $\omega_p/2\pi = 56$ Hz. Fig. 6a thus corresponds to the spectrum of surface oscillations caused by low-level external noise (mechanical vibration of the cryostat). Figs. 6b,c demonstrate the formation of the turbulent spectrum at subsequent moments of time.

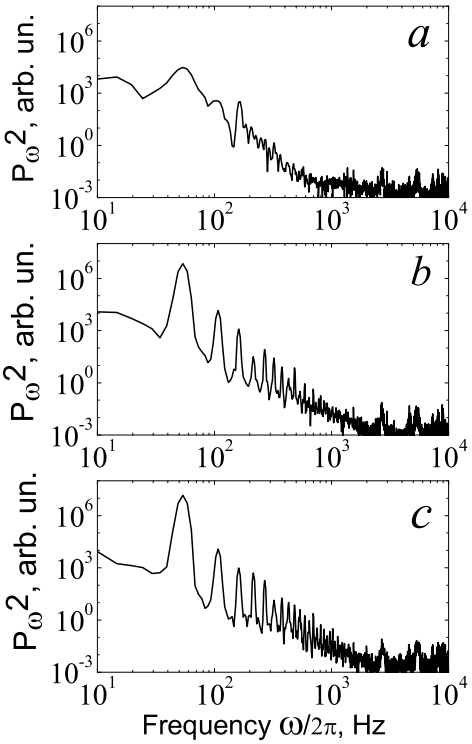

Fig. 6. Instantaneous spectra of surface oscillations calculated for different time intervals after switching on the driving force at the frequency $\omega_p/2\pi =$ 56 Hz: (a) $t = 0$ s (at the moment of time immediately before the switching on the driving force), (b) $t = 0.58$ s, and (c) $t = 1.51$ s.

It can be seen from Figs. 5 and 6 that, at each moment of time after switching the driving force off and on, the spectra of surface oscillations are similar to the steady-state spectra observed in our previous experiments at sufficiently large amplitudes. This implies that both the processes of decay,

and the processes of formation, of turbulence are controlled by the same relaxation mechanisms.

It was shown in Sec. 4.1. that the decreasing signal amplitude following removal of the driving force could be well-described by an exponential function $P(t) \sim \exp(-t/\tau)$, where τ is the effective relaxation time. The dependence of τ on frequency $\omega_p/2\pi$ is shown by open circles in Fig. 7. The straight line shows the dependence of the viscous (linear) damping time for capillary waves τ_v defined by Eq. (12), at frequency $\omega = \omega_p$, calculated from the known parameters[29] of liquid hydrogen at 15.5 K. It is clearly evident from Fig. 7 that the measured relaxation time τ for the decay of the turbulent cascade is close to the viscous damping time τ_v of the waves. The triangles in Fig. 7 shows the characteristic time of formation of turbulent cascade after switching on the driving force at the frequency range from 20 to 300 Hz. It is clear from Fig. 7 that the time of formation is close to the time of decay and to the time of viscous attenuation of the surface waves at the frequency ω_p.

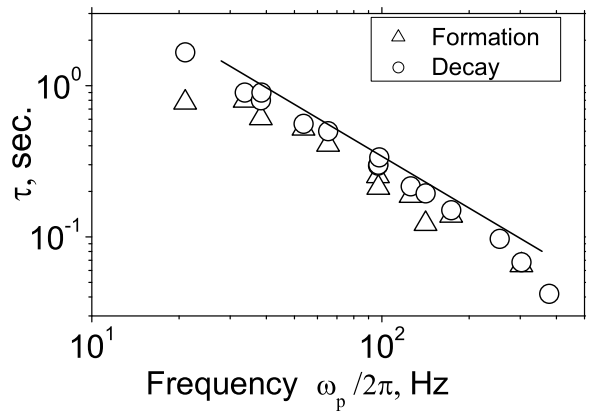

Fig. 7. Effective relaxation time τ of the surface oscillations plotted as a function of the driving frequency ω_p after removal of the driving force (open circles) and switching on the driving force (triangles). The solid line corresponds to the viscous damping time for a capillary wave τ_v of frequency $\omega = \omega_p$, calculated from known parameters of liquid hydrogen.

4.3. Suppression of High-Frequency Turbulent Oscillations of the Fluid Surface by Additional Low-Frequency Pumping

In this Section, we describe investigations of how the spectrum of capillary turbulence on the surface of liquid hydrogen evolves when an additional low-frequency pumping is switched off/on. It was found that, when the additional pumping was switched on, turbulence in the high-frequency range was suppressed and the inertial frequency range decreased. When the additional pumping was switched off, the amplitudes of high-frequency turbulent oscillations increased again and the inertial range expanded.

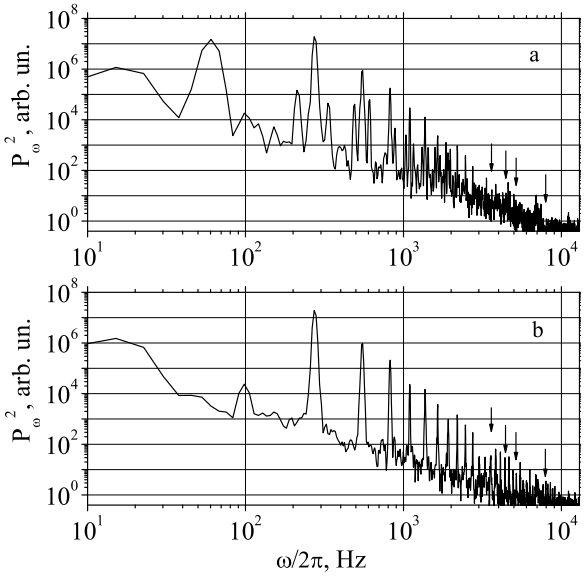

Fig. 8. Stationary spectrum of the oscillations of the fluid surface upon pumping (a) simultaneously at two resonance frequencies $\omega_1/2\pi = 61$ Hz and $\omega_2/2\pi = 274$ Hz and (b) only at the main resonant frequency $\omega_2/2\pi = 274$ Hz.

Thus there were two types of measurement. In the first, waves on the fluid surface were excited by pumping simultaneously at two different resonant frequencies of the cell. After the formation of the steady turbulent distribution, pumping at one of the frequencies (additional frequency) was stepwise switched off, whereas the intensity of pumping at the other (main) frequency remained unchanged. In measurements of the second type, waves

on the fluid surface were first excited at one of the resonant frequencies of the cell and then an additional pumping at another resonant frequency was switched on. In each case a transient process in the turbulent system of capillary waves was studied, after the additional pumping was switched off or on respectively.

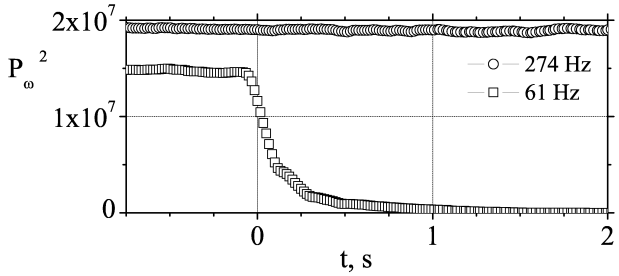

Fig. 9. Time dependence of the amplitude squared for waves on the surface of liquid hydrogen at the main (circles) and additional (squares) frequencies when the additional pumping is switched off at the time $t = 0$.

Figure 8 shows the steady-state spectra of liquid hydrogen surface oscillations before and after the additional pumping is switched off: (a) for simultaneous pumping at two resonant frequencies of the cell: main $\omega_2/2\pi = 274$ Hz and an additional $\omega_1/2\pi = 61$ Hz; and (b) after pumping at the additional frequency ω_1 is switched off. It is worth noting that the wave energy $E_{\omega_1} \propto |\eta_{\omega_1}|^2$ at the frequency ω_1 is an order of magnitude lower than the wave energy E_{ω_2} at the frequency ω_2. For this reason, the oscillation spectrum in Fig. 8a can be treated as the capillary-turbulence spectrum that is generated by the main harmonic pumping at the frequency $\omega_2/2\pi = 274$ Hz and is perturbed by the additional pumping at the frequency $\omega_1/2\pi = 61$ Hz. Correspondingly, near the relatively high peaks at frequencies that are multiples of ω_2, relatively low peaks at combination frequencies are located on both sides of the harmonics of the main frequency at a distance of the frequency ω_1 from it. The distribution in Fig. 8b is the stationary spectrum of capillary turbulence generated by the harmonic force at the frequency ω_2: the amplitude of peaks at frequencies that are multiples of the frequency ω_2 decreases in a power law as the frequency increases. It is seen that the amplitudes of the high-frequency peaks generated by pumping at one frequency (Fig. 8b) are noticeably larger than those generated by pumping at two frequencies (Fig. 8a).

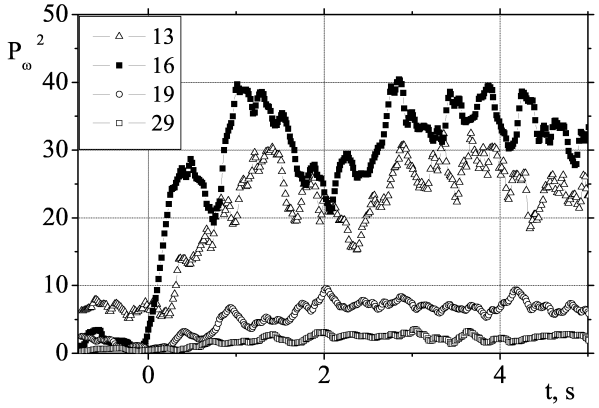

Fig. 10. Time dependence of the amplitude squared for peaks at frequencies that are multiples of the main pumping frequency ω_2 when the additional pumping at the frequency ω_1 is switched off at time $t = 0$. The triangles, closed squares, open squares, and circles correspond to the 13th (3.57 kHz), 16th (4.49 kHz), 19th (5.19 kHz), and 29th (7.96 kHz) harmonics of the main frequency ω_2, respectively. The positions of the corresponding harmonics are shown by arrows in Fig. 8.

Figure 9 shows the time dependence of the amplitude squared for waves on the surface of liquid hydrogen at the main (circles) and additional (squares) frequencies: recall that $P_\omega^2 \propto |\eta_\omega|^2$ according to Eq. (8). Pumping at the additional frequency ω_1 is switched off at time $t = 0$, whereas the pumping amplitude at the main frequency ω_2 remains unchanged. As is seen in the figure, the amplitude of the wave with the frequency ω_1 decreases almost exponentially with time and, in agreement with our previous consideration, the characteristic decay time nearly coincides with the viscous damping time $\tau_v \sim \gamma_{\omega_1}^{-1}$ of the capillary wave with the frequency ω_1.

Figure 10 shows the time dependence of the amplitude squared for peaks at frequencies that are multiples of the main pumping frequency ω_2 when the additional pumping is switched off at the time $t = 0$. The triangles, closed squares, open squares, and circles correspond to the 13th (3.57 kHz), 16th (4.49 kHz), 19th (5.19 kHz), and 29th (7.96 kHz) harmonics of the main frequency ω_2, respectively. The positions of the corresponding harmonics are shown by arrows in Fig. 8. As seen in Fig. 10, after the additional pumping is switched off, the amplitudes of the high-frequency harmonics increase by a large factor in a time comparable with the damping time for the wave at the frequency ω_1 (Fig. 9).

Analysis of the evolution of the spectrum of the fluid-surface oscillations shows that, when the additional pumping is switched on at the time $t = 0$, the amplitudes of the high-frequency oscillations decrease at $t > 0$. Thus, the observed evolution of the turbulent spectrum is completely reversible.

5. THEORETICAL CONSIDERATION OF THE DECAY OF CAPILLARY TURBULENCE

5.1. Self-similar Decay of Capillary Turbulence

We now present a brief theoretical discussion[14] of the decay of capillary turbulence on the surface of a viscous liquid after the stepwise removal of external pumping. In our subsequent analyses we suppose that the viscosity of the liquid is sufficiently small that the boundary frequency ω_b of the inertial range is much higher than the pumping frequency ω_p. In view of experimental observations and numerical calculations[10,11], it is natural to assume that the decay of turbulence is self-similar due to the significant difference between the characteristic dissipative and pumping frequency scales.

It can be shown[14] that a nonstationary self-similar solution of the kinetic equation (3) describing the decay of the turbulent cascade after the stepwise removal of external pumping (i.e. free decay) takes the following form

$$n_{\mathbf{k}} = 4\nu k_b^{-3}(t)\, g(\xi), \tag{15}$$

where $k_b(t)$ is the time-dependent high-frequency boundary of the inertial range defined in terms of wavenumber, and $g(\xi)$ is some function of the self-similar variable $\xi = k/k_b(t)$. We assume that the external pumping is stepwise switched off at time $t = 0$; i.e. $F_{\mathbf{k}}(t) = 0$ for $t \geq 0$. The numerical factor on the right-hand side of Eq. (15) is separated for the convenience of further calculations.

The substitution of Eq. (15) into kinetic equation (3) yields an equation for the self-similar function $g(\xi)$

$$-(1/4\nu)(3g(\xi) + \xi g'(\xi))k_b(t)^{-3}\dot{k}_b(t) = I(\xi) - \xi^2 g(\xi), \tag{16}$$

where the dot stands for differentiation with respect to time, the prime means differentiation with respect to the variable ξ, and $I(\xi)$ is an integral operator that is quadratic in $g(\xi)$ and is defined by the equality

$$St(n_{\mathbf{k}}(t)) = k_b(t)^{-1} I(\xi).$$

The boundary of the instantaneous inertial range $k_b(t)$ must satisfy the equation

$$k_b^{-3}\dot{k}_b = -C, \tag{17}$$

where C is a certain constant that is positive in accordance with the shift of the edge of the inertial range to lower frequencies with increasing time. From Eq. (17) it follows that

$$k_b(t) = \frac{k_b(0)}{\sqrt{1 + t/\tau}}, \tag{18}$$

where $k_b(0)$ is the position of the edge of the inertial range at the time $t = 0$ of removal of the external pumping and $\tau = 1/2Ck_b(0)$ is the characteristic turbulence decay time. The time dependence of the boundary frequency of the inertial range is described by the expression

$$\omega_b(t) = \frac{\omega_b(0)}{(1 + t/\tau)^{3/4}}, \tag{19}$$

where $\omega_b(0)$ is the initial boundary frequency. For $t \gg \tau$, the boundary frequency of the inertial range depends on time as $\omega_b(t) \sim t^{-3/4}$.

The boundary conditions for the integro-differential equation (16) have the form

$$Q_k \to 0 \quad \text{at } k \to 0, \tag{20}$$

$$g(\xi) \to 0 \quad \text{at } \xi \to \infty, \tag{21}$$

where

$$Q_k = -2\pi \int_0^k dk' k' \omega_{k'} St(n_{\mathbf{k}'}) \tag{22}$$

is the energy flux in the K space towards the larger wave number domain[17]. Condition (20) corresponds to the absence of low-frequency external pumping at $t > 0$.

Asymptotic expressions for the occupation numbers of waves found in subsequent analyses of Eqs. (15) and (16) in the case of relatively high amplitude waves, i.e. for a sufficiently wide instantaneous inertial range, are as follows:

$$n_{\mathbf{k}} = \text{const}\, k^{-3} \qquad \text{for } k \ll k_b(t) \tag{23}$$

$$n_{\mathbf{k}}(t) = \text{const}\, k_b(t)^{5/4} k^{-17/4} \qquad \text{for } k \sim k_b(t), \tag{24}$$

$$n_{\mathbf{k}}(t) = \text{const}\, k^{-3} \exp\left(-\frac{k^2}{2k_b(t)^2}\right) \qquad \text{for } k \gg k_b(t) \tag{25}$$

It can be shown by direct calculation that the solution given by Eqs. (23)–(25) satisfies the boundary conditions (20), (21).

In the experiments on the decay of capillary turbulence on the surface of liquid hydrogen described in Sec. 4.1. the relative width of the inertial range is equal to $\omega_b/\omega_p \sim 50 - 100$ at the time of removal of the external pumping.

As follows from Eqs. (7) and (11), for the case of the low-frequency noise pumping, the characteristic time of the nonlinear interaction between waves with the characteristic frequency ω is $\tau_n \sim \omega^{-1/2}$, whereas the characteristic time of the viscous damping of waves with the same frequency given by Eq. (12) is $\tau_v \sim \omega^{-4/3}$. Their ratio is $\tau_v/\tau_n \sim \omega^{-5/6}$. If, according to the results described in Sec. 4.1., we suppose that this ratio for frequencies ω on the order of the boundary frequency ω_b of the inertial range is $\tau_v/\tau_n \sim 1$, then this ratio for frequencies on the order of the pumping frequency is $\tau_v/\tau_n \sim (\omega_b/\omega_p)^{5/6} \sim 25 - 50$ at the time of the pumping removal and decreases rapidly in the process of the decay of turbulence. For the case of pumping at one resonant frequency, the stationary spectrum of capillary turbulence is given by Eq. (10). In this case the characteristic time of the nonlinear interaction is $\tau_n \sim \omega^{1/6}$, and the nonlinear-to-viscous time ratio at the pumping frequency is $\tau_v/\tau_n \sim (\omega_b/\omega_p)^{3/2} \sim 10^2 - 10^3$. Thus, even at the comparatively large ratio τ_v/τ_n, the viscosity is of significant importance for the decay of turbulence on the surface of liquid hydrogen. We see also from Eq. (24) that inside the inertial range the distribution of capillary waves is close to the stationary distribution given by (7) which is in qualitative agreement with our experimental observations described in Sec. 4.1.

5.2. Direct Numerical Study of Capillary Turbulence Decay

We have also modelled directly the decay of capillary turbulence after a stepwise removal of the driving force. The full kinetic equation (3) with a dissipative term was solved numerically. The calculations were carried out in two steps. First, the driving force was switched on and we waited for some time until a steady-state distribution has been established in the system of waves. The driving force was then removed and we observed the decay of the turbulent spectrum.

Studies of the decay of capillary turbulence formed under the action of both wide-band and narrow-band pumping have been performed. The results of calculations obtained in the case of wide-band pumping was similar to those was described in our earlier paper[10], where we used the local model of capillary turbulence.

The results of numerical calculations of the decay of turbulence following the removal of a narrow-band driving force, for times corresponding to the experimental observations in plots (a) and (b) in Fig. 5, are presented in Fig. 11. The frequency ω and the correlation function P_ω^2 are given in dimensionless units. The driving frequency was close to $\omega_p \approx 100$. It can be seen in Fig. 11 that our calculations are in qualitative agreement with the

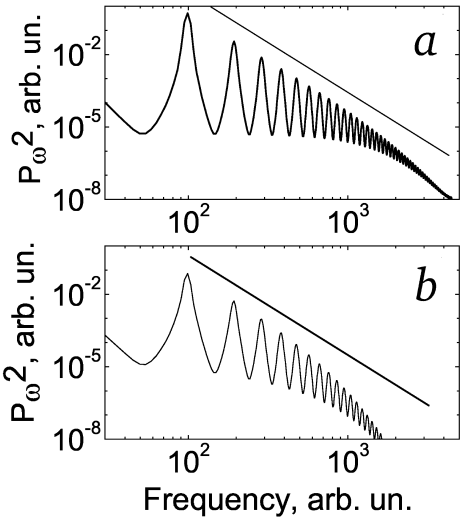

Fig. 11. Results of numerical calculations of the decay of the turbulent spectrum after the removal of the narrow-band driving force, for times corresponding to the experimental observations shown in plots (a) and (b) in Fig. 5.

experimental results (Sec. 4.1.) and theoretical analyses (Sec. 5.1.).

6. CONCLUSION

Investigations of the evolution in shape of an equipotentially charged surface of liquid in an external dc electric field have demonstrated the possibility of observing a reconstruction phenomenon – the formation of a stationary solitary wave on the flat charged surface (a hump in case of the positively charged surface of liquid hydrogen and a dimple in case of the negatively charged surface of superfluid He II). For hydrogen, it occurs at a critical value of electric field where, assuming conditions of total screening of the electric field from the bulk of the liquid by the surface charge. The critical voltage U_{c1} corresponds to the situation where the applied electric force exactly compensates the gravitational force (where the effective acceleration due to gravity tends to zero).

Measurements made with ac electric fields have permitted us to study the propagation and transformation of nonlinear capillary waves on the surface of liquid hydrogen. It has been demonstrated that a weak turbulence

state (Kolmogorov spectrum) is formed in a system of capillary waves over wide range of frequencies higher than the driving frequency ω_p.

Quasi-stationary decay of the turbulent cascade of capillary waves has been observed experimentally on the liquid-hydrogen surface after a stepwise switching-off of the low-frequency pumping. The decay starts from high frequencies and ends close to the reciprocal viscous-damping time of a wave at the pump frequency. The energy-containing part of the spectrum (maximum of the distribution I_ω) is retained at low frequencies during the entire decay process. This indicates that viscous losses at all frequencies are of central importance for the correct interpretation of decay processes in such a system of nonlinearly interacting capillary waves. Observations of the formation of the cascade and the results of analytical studies of self-similar decay of turbulence, as well as of direct numerical modelling, are in satisfactory agreement with those conclusions.

Relaxation of the turbulent oscillations on the surface of liquid hydrogen has been studied for the case where an additional low-frequency perturbation is switched on/off. For the case of spectrally narrow pumping it was found that, after the additional pumping was switched off, the wave amplitudes in the high-frequency part of the turbulent spectrum increased, thereby causing the inertial frequency range to expand. The observed evolution of the spectrum is reversible: after the additional perturbation is switched on, the wave amplitudes in the high-frequency part of the turbulent spectrum decrease and the inertial range narrows. It has thus been shown that high-frequency turbulent oscillations on the liquid surface can be suppressed by the addition of an extra low-frequency pump force.

Acknowledgements

We are grateful to V. E. Zakharov, E. A. Kuznetsov, M. T. Levinsen, A. I. Dyachenko, and V. B. Efimov for the interest and valuable discussions, and to V. N. Khlopinski for assistance in preparing the experiments. The investigations were supported by the Russian Foundation for Basic Research, project Nos. 05-02-17849 and 06-02-17253, by the Presidium of the Russian Academy of Sciences in frames of the programs "Quantum Macrophysics" and "Mathematical Methods in Nonlinear Dynamics", and by the Engineering and Physical Sciences Research Council (UK).

REFERENCES

1. A. A. Levchenko and L. P. Mezhov-Deglin, *Low Temp. Phys.* **22**, 162 (1996).

2. A. A. Levchenko, E. Teske, G. V. Kolmakov, P. Leiderer, L. P. Mezhov-Deglin, and V. B. Shikin, *JETP Lett.* **65**, 572 (1997).
3. A. A. Levchenko, G. V. Kolmakov, L. P. Mezhov-Deglin, M. G . Mikhailov, and A. B. Trusov, *Low Temp. Phys.* **25**, 242 (1999).
4. A. A. Levchenko, G. V. Kolmakov, L. P. Mezhov-Deglin, M. G. Mikhailov, and A. B. Trusov, *J. Low Temp. Phys.* **119**, (3/4), 343 (2000).
5. M. Yu. Brazhnikov, A. A. Levchenko, G. V. Kolmakov, and L. P. Mezhov-Deglin, *JETP Lett.* **73**, 398 (2001).
6. M. Yu. Brazhnikov, A. A. Levchenko, G. V. Kolmakov, and L. P. Mezhov-Deglin, *Low Temp. Phys.* **27**, 876 (2001).
7. M. Yu. Brazhnikov, A. A. Levchenko, G. V. Kolmakov, and L. P. Mezhov-Deglin, *JETP Lett.* **74**, 583 (2001).
8. M. Yu. Brazhnikov, A. A. Levchenko, and L. P. Mezhov-Deglin, *Instr. Exp. Techn.* **45** (6), 758 (2002).
9. M. Yu. Brazhnikov, A. A. Levchenko, G. V. Kolmakov, *JETP* **95**, 447, (2002).
10. G. V. Kolmakov, A. A. Levchenko, M. Yu. Brazhnikov, L. P. Mezhov-Deglin, A. N. Silchenko, and P. V. E. McClintock, *Phys. Rev. Lett.* **93** (7), 074501 (2004).
11. M. Yu. Brazhnikov, G. V. Kolmakov, A. A. Levchenko, L. P. Mezhov-Deglin, A. N. Silchenko, and P. V. E. McClintock, *JETP Lett.* **80** (2), 90 (2004).
12. M. Yu. Brazhnikov, G. V. Kolmakov, A. A. Levchenko, L. P. Mezhov-Deglin, and P. V. E. McClintock, *J. Low Temp. Phys.* **139** (5/6), 523 (2005).
13. M. Yu. Brazhnikov, G. V. Kolmakov, A. A. Levchenko, and L. P. Mezhov-Deglin, *JETP Lett.* **82** (9), 565 (2005).
14. G. V. Kolmakov *JETP Lett.* **83** (2), 58 (2006).
15. L. P. Gor'kov and D. M. Chernikova, *Doklady Akad. Nauk S.S.S.R.* **228**, 829 (1976).
16. L. D. Landau and E. M. Lifshitz, *Course of Theoretical Physics, Vol. 6: Fluid Mechanics* (Pergamon, New York, 1987; Nauka, Moscow, 1988).
17. V. Zakharov, V. L'vov, and G. Falkovich, *Kolmogorov Spectra of Turbulence I* (Springer-Verlag, Berlin, 1992).
18. V. E. Zakharov, *Zh. Prikl. Mech. Techn. Fiz.* **2**, 89 (1968) [Engl. transl.: *J. Appl. Mech. Tech. Phys.*].
19. V. E. Zakharov and N. N. Filonenko, *Zh. Prikl. Mekh. Tekh. Fiz.* **5**, 62 (1967) [Engl. transl.: *J. Appl. Mech. Tech. Phys.*].
20. W. Wright, R. Hiller, and S. Putterman, *J. Acoust. Soc. Am.* **92**, 2360 (1992).
21. E. Henry, P. Alstrom, and M. T. Levinsen, *Europhys. Lett.* **52**, 27 (2000).
22. M. Lommer and M. T. Levinsen, *J. Fluoresc.* **12**, 45 (2002).
23. M. Yu. Brazhnikov, G. V. Kolmakov, A. A. Levchenko, L. P. Mezhov-Deglin, *Europhys. Lett.* **58** (4), 510 (2002).
24. A. N. Pushkarev and V. E. Zakharov, *Phys. Rev. Lett.* **76**, 3320 (1996).
25. A. N. Pushkarev and V. E. Zakharov, *Physica D* (Amsterdam) **135**, 98 (2000).
26. C. Connaughton, S. Nazarenko, A. Pushkarev, *Phys. Rev. E* **63** (4), 046306 (2001).
27. G. E. Falkovich and A. B. Shafarenko, *Sov. Phys. JETP* **67**, 1393 (1988).
28. S. Mallat, *A Wavelet Tour of Signal Procesing* (Academic Press, New York, 1997).
29. *The Properties of Condensed Phases of Hydrogen and Oxygen*, Ed. by

Nonlinear Phenomena at the Surface of Liquid Hydrogen

B. I. Verkin (Naukova Dumka, Kiev, 1984) [in Russian].